Synthetic Peptides from Mouse Fc Receptor (MoFc$_\gamma$RII) That Alter the Binding of IgG to MoFc$_\gamma$RII[†]

Edie Bowles Goldsmith,[‡] Bruce W. Erickson, and Nancy L. Thompson*

Department of Chemistry, University of North Carolina, Chapel Hill, North Carolina 27599-3290

Received June 28, 1996; Revised Manuscript Received October 22, 1996[⊗]

ABSTRACT: Fc receptors are transmembrane proteins, found on the surfaces of immune cells, that aid in the removal of foreign pathogens by binding to antibody-coated targets via the Fc regions of the antibodies. Using peptides synthesized on pins, overlapping dodecapeptides (170) were synthesized to cover the extracellular region of the mouse Fc receptor for IgG, moFc$_\gamma$RII. The peptides were screened for antibody binding activity by using multivalent immune complexes composed of anti-dinitrophenyl monoclonal mouse IgG1 (ANO6) and dinitrophenyl conjugated to human serum albumin (DNP-HSA). Assays were also carried out with an anti-moFc$_\gamma$RII monoclonal rat IgG (2.4G2). The peptides that interacted with these antibodies prompted the synthesis of two soluble peptides: peptide A [Fc$_\gamma$RII-(108−119), RCHSWRNKLLNRamide] and peptide B [Fc$_\gamma$RII-(153−165), CKGSLGRTLHQSKamide]. Monomeric S-alkylated (A, B), homodimeric (AA, BB), heterodimeric (AB), and scrambled homodimeric (CC, DD) forms of these peptides were synthesized and examined for their ability to inhibit immune-complex binding to immobilized soluble Fc$_\gamma$RII. Peptides AA and CC completely inhibited immune-complex binding while each of the other peptides partially inhibited binding (AB, 80%; A, 80%; BB, 65%; DD, 64%; B, 52%). The pair of monomeric moFc$_\gamma$RII peptides and the set of five dimeric peptides showed the same increase in binding inhibition with increasing net positive charge per residue. These results suggest that the Fc region of IgG binds to the solvent-exposed B/C and F/G loops of the moFc$_\gamma$RII receptor through predominantly electrostatic forces.

The cell surface IgG receptor, Fc$_\gamma$RII,[1] is present on a variety of cell types including macrophages, monocytes, lymphocytes, and neutrophils and is thought to mediate a number of immune functions, including phagocytosis and B cell regulation (Mellman et al., 1988; Kinet, 1989; Ravetch & Kinet, 1991). Mouse Fc$_\gamma$RII (moFc$_\gamma$RII) is a single, transmembrane-spanning glycoprotein with a molecular weight of 47 000−70 000 (Unkeless et al., 1981). A member of the immunoglobulin gene superfamily, it contains two intrachain disulfide-bridged domains that each have two sites for N-linked glycosylation (Williams & Barclay, 1988; Hibbs et al., 1988). MoFc$_\gamma$RII binds monomeric IgG1, IgG2a, and IgG2b with low affinity ($K_a \sim 10^5$ M^{-1}), binds aggregated IgG1, IgG2a, and IgG2b with an increased affinity ($K_a \sim 5 \times 10^6$ to 5×10^7 M^{-1}), and cross-reacts with human IgG1 and human IgG3 (Burton, 1985; Ravetch & Kinet, 1991).

To identify sites on moFc$_\gamma$RII that bind to the Fc region of IgG, a series of 170 overlapping dodecapeptides was constructed on pins using solid-phase peptide synthesis (Geysen et al., 1984) and assayed for binding to IgG immune complexes. Two moFc$_\gamma$RII regions from the membrane-adjacent IgG domain of the receptor were identified that possessed high propensities for immune-complex binding. They are disulfide-bridged in the native protein and contain residues thought to be located in solvent-accessible loop regions. To confirm the involvement of these moFc$_\gamma$RII regions in IgG binding, several soluble peptides based on moFc$_\gamma$RII were synthesized and purified by conventional methods. Subsequent measurements with immobilized receptors and solution-phase immune complexes demonstrated the ability of these soluble peptides to alter the interaction of IgG and moFc$_\gamma$RII. The effects of the peptides on the IgG−moFc$_\gamma$RII interaction were different for monomeric, homodimeric, and heterodimeric forms of these moFc$_\gamma$RII peptides.

MATERIALS AND METHODS

Cells. Chinese hamster ovary (CHO) cells, which were transfected with the gene for and secrete a soluble form of the mouse receptor moFc$_\gamma$RII, called sFc$_\gamma$RII (Qu et al., 1988), were a kind gift from J. C. Unkeless (Mount Sinai School of Medicine). ANO6, a mouse−mouse hybridoma which produces anti-dinitrophenyl (DNP) IgG1 antibodies (Leahy et al., 1988), was obtained from H. M. McConnell (Stanford University). 2.4G2, a rat−mouse hybridoma which produces antibodies specific for moFc$_\gamma$RII (Unkeless, 1979), was provided by B. Diamond (Albert Einstein College of

[†] This work was supported by NIH Grants GM-37145 (N.L.T.) and GM-42031 (B.W.E.) and by NSF Grant GER-9024028 (N.L.T.).

* To whom correspondence should be addressed. Telephone: (919) 962-0328. Fax: (919) 962-2388. Email: nlt@unc.edu.

[‡] Present address: Department of Biological Sciences, University of South Carolina, Columbia, SC 29208.

[⊗] Abstract published in *Advance ACS Abstracts,* December 15, 1996.

[1] Abbreviations: 2.4G2, anti-(mouse Fc$_\gamma$RII) rat IgG monoclonal antibody; ANO6, anti-dinitrophenyl mouse IgG1 monoclonal antibody; BSA, bovine serum albumin; CHO, Chinese hamster ovary; DCM, dichloromethane; DIEA, diisopropylethylamine; DNP, 2,4-dinitrophenyl; DNP-HSA, dinitrophenyl-human serum albumin; DTT, dithiothreitol; ELISA, enzyme-linked immunosorbent assay; Fc$_\gamma$RII, Fc IgG receptor; Fmoc, 9-fluorenylmethoxycarbonyl; HOBt, 1-hydroxybenzotriazole; MAR18.5, anti-(rat κ light chain) antibody; NEM, *N*-ethylmaleimide; NMP, *N*-methylpyrrolidinone; PBS, phosphate-buffered saline; PBSA, phosphate-buffered saline with sodium azide; PBST, phosphate-buffered saline with Tween-20; sFc$_\gamma$RII, soluble Fc IgG receptor; TB, *N*-[tris(hydroxymethyl)methyl]-2-aminoethanesulfonic acid buffer; TCEP, tris(carboxyethyl)phosphine; TFA, trifluoroacetic acid.

S0006-2960(96)01564-4 CCC: $14.00

Medicine). CHO cells were maintained in DMEM-H supplemented with 5% fetal calf serum, 2.0 μM methotrexate (Sigma Chemical Co., St. Louis, MO), 100 IU/mL penicillin, 100 μg/mL streptomycin, and 0.1 mM nonessential amino acids (Gibco Laboratories, Grand Island, NY). Hybridomas were grown in DMEM/F12 supplemented with 1 mM sodium pyruvate, 2 mM L-glutamine, 100 IU/mL penicillin, 100 μg/mL streptomycin, and fetal calf serum (ANO6, 5%; 2.4G2, 10%).

Proteins. Polyclonal rat and sheep IgG (Sigma) were dissolved in phosphate-buffered saline (PBS; 0.05 M sodium phosphate, 0.15 M sodium chloride, pH 7.4) containing 0.01% sodium azide (PBSA). Horseradish peroxidase conjugates of goat anti-(rat IgG) IgG and goat anti-(mouse IgG) IgG (Sigma), mouse $F(ab')_2$ IgG (Jackson ImmunoResearch Laboratories, Inc., West Grove, PA), and epitope scanning test antibody (Cambridge Research Biochemicals, Inc., Wilmington, DE) were reconstituted according to the manufacturers' recommendations. 2.4G2 antibodies were purified from cell supernatants by affinity chromatography with anti-(rat κ light chain) antibody MAR18.5 (Poglitsch & Thompson, 1990). $sFc_\gamma RII$ was purified from cell culture supernatants by affinity chromatography with 2.42G Fab (Gesty-Palmer & Thompson, 1997). Bovine serum albumin (BSA) and DNP-conjugated human serum albumin (DNP-HSA) were obtained commercially (Sigma).

ANO6 antibodies were purified from cell supernatants by affinity chromatography using DNP-HSA as previously described (Pisarchick & Thompson, 1990), except that the N-DNP-glycine used for elution was separated from the antibodies by gel filtration using Sephadex G-50 in PBSA followed by dialysis against PBSA. Immune complexes were formed by combining (24 h, 4 °C) ANO6 and DNP-HSA (Mellman & Plutner, 1984). Multiple concentrations of ANO6 (0.78−0.003 mg/mL) and DNP-HSA (0.8−0.003 mg/mL) were initially tested for immune-complex formation. Complex size was judged spectrophotometrically by examining the ability of generated complexes to scatter light. Four complexes were further examined for their ability to bind immobilized $Fc_\gamma RII$, and, of these, complexes formed from ANO6 (25 μg/mL) and DNA-HSA (50 μg/mL) in PBS containing 0.5 mg/mL BSA were chosen.

Synthesis of Peptides on Pins. Pins (Cambridge Research Biochemicals) were obtained as polyethylene rods graft-polymerized by γ-irradiation with acrylic acid to yield a poly(acrylic acid) surface to which a peptide-like spacer consisting of hexamethylenediamine and *N*-(9-fluorenylmethoxycarbonyl)-β-alanine (Fmoc-β-alanine) had been coupled (Geysen et al., 1987). The sequence of $moFc_\gamma RII$ (Ravetch et al., 1986) was used to construct all possible overlapping dodecapeptides on separate pins using previously described techniques (Geysen et al., 1984; James & Harley, 1992).

Removal of the Fmoc amino-protecting group was accomplished by immersing the pin heads in a solution of piperidine (20 mL) and *N*-methylpyrrolidinone (NMP; 80 mL) for 30 min. Pins were washed with 120-mL volumes of the following solvents: NMP (5 min), methanol (4 times, 2 min), and NMP (2 min). While the pins were drying, Fmoc-amino acids (Cambridge Research Biochemicals) were dissolved in a solution of 1-hydroxybenzotriazole (HOBt, 222 mg) in NMP (50 mL) to final concentrations of 30−35 mM. The wells of a 96-well plate were filled with appropriate amino acid solutions (150 μL) and the coupling reactions were allowed to proceed overnight. During the synthesis, the four cysteines in $moFc_\gamma RII$ were replaced by alanine residues. The deprotection, washing, and coupling procedures were repeated 11 times. After removal of the final Fmoc protecting group, the N-terminal amino group was acetylated by incubating the pins in a 50:5:1 (v/v/v) solution of NMP, acetic acid, and diisopropylethylamine (DIEA) for 90 min at room temperature. Side-chain deprotection was accomplished using a 1:1:38 (v/w/v) solution of ethanedithiol, phenol, and trifluoroacetic acid (TFA) for 4 h. Final washings were performed using 120-mL volumes of dichloromethane (DCM; twice, 2 min), DIEA/DCM 6:114 (v/v) (twice, 2 min), and DCM (5 min). Pins were air-dried (20 min), rinsed in distilled water (2 min), rinsed in methanol (18 h), and dried in an evacuated desiccator for storage.

ELISA Assays of Peptides on Pins. An enzyme-linked immunosorbent assay (ELISA) was used to judge the binding of immune complexes and 2.4G2 to the peptides on pins (Kemeny, 1991). All assays were carried out in 96-well microtiter plates (Costar, Cambridge, MA) with PBS as a buffer and with 175 μL/well unless otherwise noted. To block nonspecific binding, pins were incubated with 10 mg/mL BSA (1 h, 4 °C). Pins were soaked in PBS containing 0.05% Tween 20 (PBST) while microtiter plates were washed three times in PBST with moderate shaking. Sheep IgG (0.1−0.2 mg/mL) was added to each well as an additional inhibitor of nonspecific binding (1 h, 4 °C). After being washed with PBST, pins were treated (1 h, 4 °C) with immune complexes, mouse IgG $F(ab')_2$ (0.023 mg/mL), monomeric 2.4G2 (0.023 mg/mL), or rat IgG (0.023 mg/mL). A PBST wash preceded treatment with horseradish peroxidase conjugates of goat anti-(rat IgG) IgG and/or goat anti-(mouse IgG) IgG prepared at a 1:500 dilution in PBST with 0.5 mg/mL BSA (1 h, 4 °C).

After a final PBST wash, pins were incubated (40 min, 25 °C) with 175 μL of *o*-phenylenediamine dihydrochloride (0.4 mg/mL) in citrate−phosphate buffer (0.05 M sodium citrate, 0.15 M sodium phosphate, pH 5.0) containing 20 μL of 30% hydrogen peroxide. The enzymatic reaction was quenched with 2 M sulfuric acid (88 μL) and the absorbance was read at 490 nm (Molecular Devices Vmax Kinetic Microplate Reader, Menlo Park, CA). For the experimental conditions used, the absorbance of this plate reader was linear for concentrations up to OD $\approx$ 3.0.

Pins were cleaned after each assay by soaking in 8 M urea and then sonicating (30 min, 60 °C) in a solution of 0.1 M sodium phosphate, 1% sodium dodecyl sulfate, and 1% β-mercaptoethanol at pH 7.2. Pins were washed (2 min, 55−60 °C) several times with distilled water, washed (20 min, 25 °C) with methanol, allowed to air-dry, and stored under vacuum with a desiccant.

Synthesis, Modification, and Purification of Soluble Peptides. Monomeric peptides A (RCHSWRNKLLNRamide) and B (CKGSLGRTLHQSKamide) and the scrambled peptides C (RCRLRNWSLNKHamide) and D (CGHLSRKLKQTGSamide) were synthesized by the UNCCH-NIEHS Protein Chemistry Laboratory. Peptides C and D were identical to A and B, respectively, in amino acid composition but differed in amino acid sequence, except that the positions of the cysteine residues were preserved.

The cysteine residue of peptide A or B was modified by reduction with tris(carboxyethyl)phosphine (TCEP; Molec-

ular Probes Inc., Eugene, OR) and alkylation with *N*-ethylmaleimide (NEM, Sigma) (Burns et al., 1991). A solution of peptide (1 molar equiv) and TCEP (0.8 molar equiv) in 20 mM sodium acetate buffer (pH 4.5) was kept at 25 °C for 15 min. Excess NEM (25 molar equiv) was added, and the solution was kept at room temperature for 21 h and then lyophilized. The dried peptide was washed with several small volumes of ethyl ether to remove unreacted NEM and was purified by HPLC. When the S-alkylated peptide was assayed using Ellman's reagent (Sigma) as previously described (Habeeb, 1972), no free sulfhydryl groups were detected.

Each synthetic peptide was dissolved in a minimum volume of 0.05% TFA in water, injected onto a C_{18} reverse-phase HPLC column (1 × 25 cm; Synchropak RP-P, Synchrom, Inc., Lafayette, IN), and eluted with a 0−21% gradient of acetonitrile in water containing 0.05% TFA at a flow rate of 4 mL/min. Eluted peptides were detected by measuring the absorbance at 225 or 280 nm and were rechromatographed on another C_{18} reverse-phase column (1 × 25 cm, Vydac 218TP1010; Vydac, Hesperia, CA) using the same gradient. Like fractions were pooled and lyophilized. Peptides were stored over desiccant at 4 °C. Quantitative amino acid analysis was used to verify the expected amino acid composition and to determine peptide concentration.

Formation of the AB Heterodimer. A heterodimeric peptide was constructed (Shaw et al., 1987). Peptide A (12 mg) was dissolved in a solution of 20 mM *N*-[tris(hydroxymethyl)methyl]-2-aminoethanesulfonic acid and 1 mM ethylenediaminetetraacetic acid (TB, pH 6.5). 175 mM dithiothreitol (DTT) in 50 mM sodium borate (800 μL; pH 8.8) was added under argon to give a final concentration of 50 mM DTT. Following reduction of peptide A (22 h, argon), excess DTT was removed by gel filtration chromatography using Sephadex G-10 and deoxygenated TB. To form the mixed disulfide of peptide A with pyridine-2-thiol, 0.5 M 2,2′-dithiodipyridine (Aldrithiol-2; Aldrich Chemical Co., Milwaukee, WI) in ethanol (35 μL) was added to the eluted peptide and incubated under argon for 25 min. The mixed disulfide was separated from 2-thiopyridone and 2,2′-dithiodipyridine by Sephadex G-10 chromatography in deoxygenated TB. Fractions containing the mixed disulfide were purged with argon and stored at 4 °C.

Peptide B was reduced as described above for peptide A. After Sephadex G-10 chromatography, a 10% molar excess of reduced B was combined with the A mixed disulfide, and the solution was kept under argon for 21 h. Affinity chromatography on thiopropyl-Sepharose in deoxygenated TB to remove unreacted B was followed by gel filtration on Sephadex G-10 in deoxygenated TB to separate the AB heterodimer from 2-thiopyridone. The AB heterodimer was purified by reverse-phase HPLC using the Vydac C_{18} column, and its composition was confirmed by quantitative amino acid analysis.

Competitive ELISA. Competitive binding measurements were carried out with mixtures of immune complexes and soluble peptides using an ELISA to monitor inhibition by the peptides of the binding of the immune complexes to immobilized sFc$_\gamma$RII. Microtiter plate wells (Becton Dickinson, Oxnard, CA) were incubated overnight at 4 °C with sFc$_\gamma$RII (10 μg/mL) in PBS. ELISA measurements were carried out as described above, except that the peptide−immune complex solution was incubated for 30 min at room temperature prior to use, the sample volumes were 100 μL/well for all steps except the blocking incubation (150 μL/well), and sheep IgG was omitted as an additional blocker for nonspecific binding.

RESULTS

Identification of MoFc$_\gamma$RII Peptides on Pins That Bind to Immune Complexes. To identify possible binding sites on moFc$_\gamma$RII for IgG, a library of overlapping dodecapeptides covering the extracellular sequence of moFc$_\gamma$RII was synthesized on pins. These peptides on pins were tested for binding to immune complexes by ELISA (Figure 1A). In these assays, the primary antibody was immune complexes formed from the mouse IgG1 anti-DNP monoclonal antibody ANO6 and DNP-HSA. Immune complexes were used because the interaction of monomeric mouse IgG with moFc$_\gamma$RII is weak ($K_a \approx 10^5\ M^{-1}$). The secondary antibody was horseradish peroxidase-conjugated goat anti-(mouse IgG) IgG, which was expected to have minimal interactions with moFc$_\gamma$RII pin peptides because of the weak binding of IgG to moFc$_\gamma$RII. To measure nonspecific binding, assays in which the primary antibody was polyclonal mouse F(ab)′$_2$ IgG were also carried out (Figure 1B). The F(ab)′$_2$ antibody fragment lacks the Fc region and should not interact specifically with peptides derived from moFc$_\gamma$RII.

To correct for nonspecific binding, the immune complex (Figure 1A) and the mouse F(ab)′$_2$ IgG data (Figure 1B) were separately averaged, and the ratio of these two averages was used to scale the nonspecific mouse F(ab)′$_2$ data to the immune-complex data. Subtraction of the scaled F(ab)′$_2$ data from the immune-complex data (Figure 1C) revealed that pin peptides 108 and 155 from the membrane-adjacent Ig domain of moFc$_\gamma$RII reacted well with the immune complexes. Dodecapeptide 108 (RAHSWRNKLLNR, residues 108−119) belongs to the cluster of pin peptides 101−111 with significant immune-complex binding activity. This cluster spans a region consisting of residues 101−122 and includes alanine substituted for Cys^{109}, which participates in the disulfide bond of the membrane-adjacent Ig domain of native moFc$_\gamma$RII. Dodecapeptide 155 (GSLGRTLHQSKP, residues 155−166) belongs to the cluster of pin peptides 150−159 with significant immune-complex binding activity. This cluster spans a region consisting of residues 150−170 and contains alanine substituted for Cys^{153}, which also participates in the Cys^{109}−Cys^{153} disulfide bond of the membrane-adjacent domain of native moFc$_\gamma$RII.

Identification of MoFc$_\gamma$RII Peptides on Pins That Bind to Monomeric Anti-MoFc$_\gamma$RII Antibody 2.4G2. To further examine if these two regions of moFc$_\gamma$RII contain IgG binding sites, the anti-moFc$_\gamma$RII monoclonal rat antibody 2.4G2 was tested for binding to the pin peptides (Figure 2A). This antibody inhibits the binding of IgG to moFc$_\gamma$RII when bound to the receptor through its Fab region (Unkeless, 1979). Since 2.4G2 binds tightly to the receptor ($K_a \approx 10^9\ M^{-1}$) (Poglitsch & Thompson, 1990), the monomeric form of this antibody was used. Monomeric polyclonal rat IgG was used as a control for nonspecific binding since neither its Fab nor its Fc region should have strong affinity for the receptor (Figure 2B). The secondary antibody used was horseradish peroxidase-conjugated goat anti-(rat IgG) IgG.

To correct for nonspecific binding, the 2.4G2 data (Figure 2A) and the polyclonal rat IgG data (Figure 2B) were

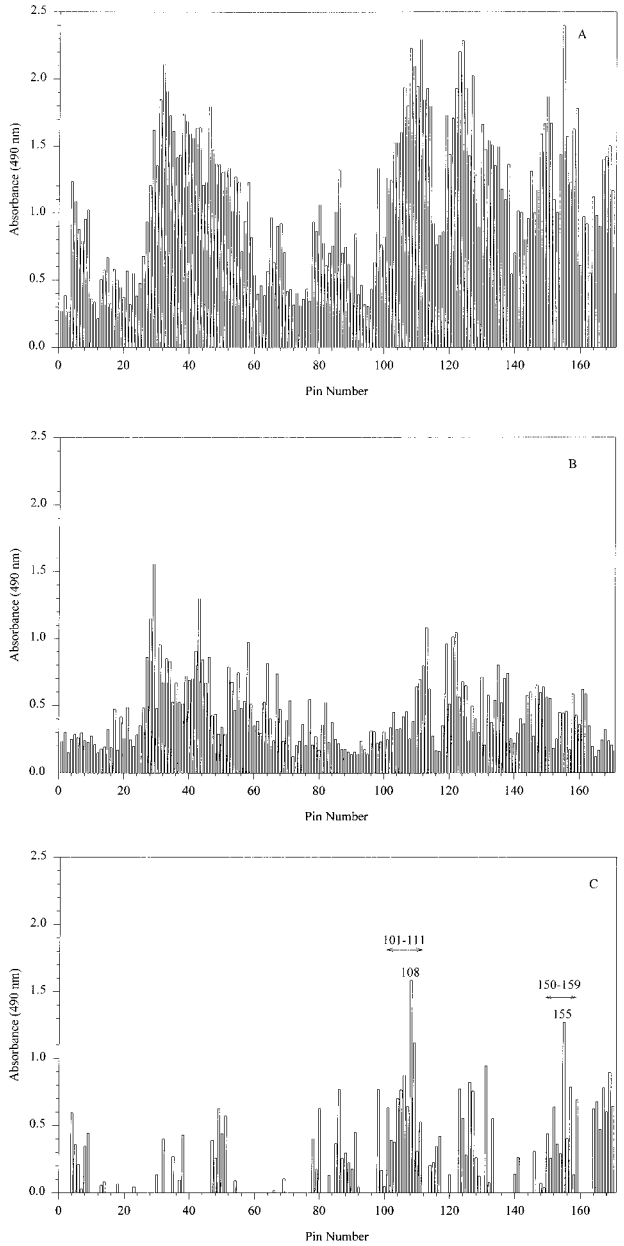

FIGURE 1: Binding of mouse IgG1 immune complexes to moFc$_\gamma$-RII peptides on pins. Bars represent the average absorbance at 490 nm of three trials for binding of (A) mouse IgG1 immune complexes or (B) mouse IgG F(ab′)$_2$ antibody fragments to moFc$_\gamma$-RII dodecapeptides on pins. To correct for nonspecific binding, the average of the immune-complex data in (A) was divided by the average of the IgG F(ab′)$_2$ data in (B), and this ratio was multiplied by the IgG F(ab′)$_2$ data to scale it to the immune-complex data. Panel C shows the results of subtracting each scaled IgG F(ab′)$_2$ data point from the comparison immune-complex data point; negative values are shown as zero.

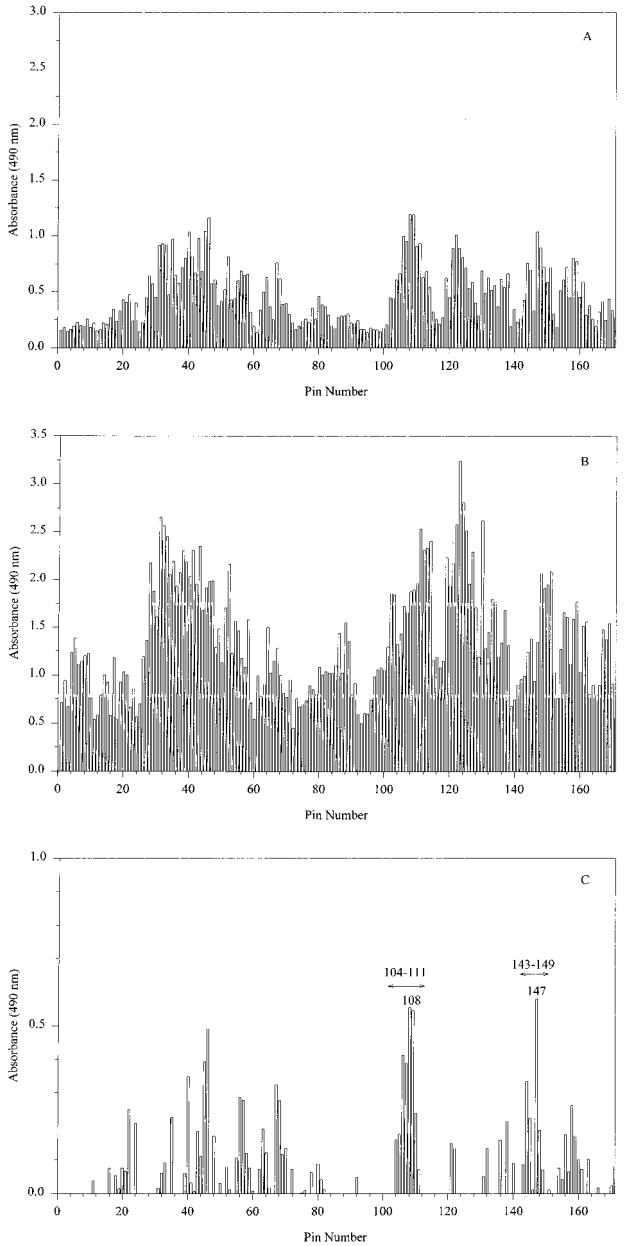

FIGURE 2: Binding of anti-Fc$_\gamma$RII antibody 2.4G2 to moFc$_\gamma$RII peptides on pins. Bars represent the average absorbance at 490 nm of three trials for binding of (A) anti-Fc$_\gamma$RII monoclonal rat IgG 2.4G2 or (B) nonspecific polyclonal rat IgG to moFc$_\gamma$RII dodecapeptides on pins. To correct for nonspecific binding, the average of the 2.4G2 data in (A) was divided by the average of the data for the polyclonal rat IgG in (B), and this ratio was multiplied by the polyclonal rat IgG data to scale it to the 2.4G2 data. Panel C shows the results of subtracting each scaled polyclonal rat IgG data point from the corresponding 2.4G2 data point; negative values are shown as zero.

separately averaged, and the ratio of these two averages was used to scale the polyclonal rat IgG data to the 2.4G2 data. Subtraction of the scaled rat polyclonal IgG data from the 2.4G2 data (Figure 2C) revealed several regions of binding. Two of these regions overlapped the regions that interacted with the immune complexes. The two regions included pin peptides 104−111 and 143−149, which encompass residues 104−122 and 143−160, respectively. The most active peptide from the first region, pin peptide 108, is identical to the most active peptide from this region found with the immune complexes. The most active peptide from the second region, pin peptide 147 (HSGDYYAKGSLG, residues 147−158), shares four residues (GSLG) with pin peptide 155, the most active peptide from this region found with the immune complexes.

Charge Analysis of Peptides on Pins. The two pin peptides that bound most tightly to the immune complexes have a high net positive charge. The net charge for each of the 170 pin peptides was calculated, for the physiological pH of the ELISA measurements (pH 7.4), as the sum of the charges on the side chains of the Asp and Glu residues (−1 each) and the Lys and Arg residues (+1 each) (Figure 3A). Because the pin peptides were acetylated at the N terminus and attached to the pin by an amide bond at the C terminus,

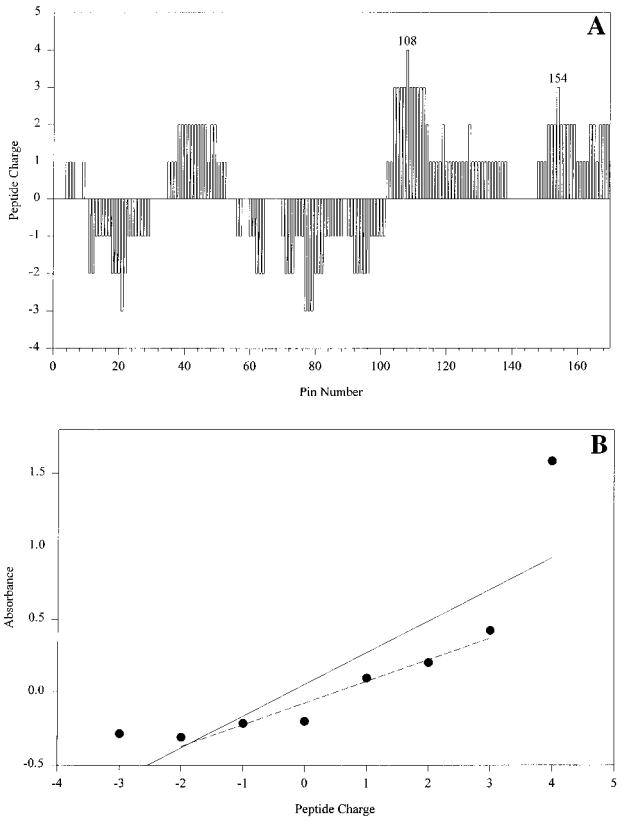

FIGURE 3: Correlation between net charge and immune complex binding of peptides on pins. (A) This plot shows the net charge at pH 7.4 of each acetylated dodecapeptide bound to the pin by an amide bond. (B) This plot shows the average absorbance at 490 nm for each set of peptides from Figure 1C with a given charge. The solid line is the least-squares line of best fit through all eight points and has a correlation coefficient of 0.84. The dashed line is the least-squares line of six points where the −3 and +4 points, which are represented by fewer than 10 pins, are excluded and has a correlation coefficient of 0.97. The values of P_N for these correlation coefficients given the numbers of points in the data sets *(N)* are 0.017 and 0.014, respectively.

these moieties did not contribute to the net charge of the peptides. Pin peptides 1−90 from the first Ig domain of moFc$_\gamma$RII have net charges ranging from −3 to +2. In contrast, pin peptides 91−169 from the second Ig domain are mostly positively charged, including those from the two regions that bound most tightly to the immune complexes (Figure 1C). Figure 3B demonstrates a positive correlation between the average binding of immune complexes to sets of pin peptides having the same net charge and the net charge of each set. The greater the net positive charge, the greater the average binding.

Effect of Soluble Peptides on Binding of IgG1 to MoFc$_\gamma$RII. To study further the effect of the most active peptides identified by the pin method on the interaction of moFc$_\gamma$RII with IgG1, several soluble peptides were synthesized using conventional solid-phase techniques and were purified by HPLC. Dodecapeptide A corresponds to pin dodecapeptide 108, and tridecapeptide B corresponds to pin peptide 154, which contains 11 of 12 residues from pin peptide 155 and five residues from pin peptide 147, plus Cys^{153} at the N terminus. Air oxidation and HPLC purification gave the homodimeric 24-residue peptide AA and the 26-residue peptide BB, respectively. Also, the cysteine residues of monomeric peptides A and B were modified with NEM to prevent air oxidation to the dimers AA and BB, respectively.

Table 1: Seven Soluble Synthetic Peptides

Peptide	Residues	Sequence[a]	Net Charge at pH 7.4[b]	Number of Residues	Net Charge per Residue (%)
A	(108-119)	RCHSWRNKLLNR | X	+5	12	42
AA	(108-119)$_2$	RCHSWRNKLLNR | RCHSWRNKLLNR	+10	24	42
B	(153-165)	CKGSLGRTLHQSK | X	+4	13	31
BB	(153-165)$_2$	CKGSLGRTLHQSK | CKGSLGRTLHQSK	+8	26	31
AB	(108-119)(153-165)	RCHSWRNKLLNR | CKGSLGRTLHQSK	+9	25	36
CC	Scrambled (108-119)$_2$	RCRLRNWSLNKH | RCRLRNWSLNKH	+10	24	42
DD	Scrambled (153-165)$_2$	CGHLSRKLKQTGS | CGHLSRKLKQTGS	+8	26	31

[a] Each peptide chain had a free amino group at its N terminus and an amide group (CO−NH$_2$) at its C terminus. For S-alkylated peptides A and B, X is the *S*-(*N*-ethyl-2-succinimidyl) group resulting from the addition of the cysteine thiol group to the double bond of NEM. [b] Scored as +1 for the N-terminal amino group and each Lys and Arg residue; no Asp or Glu residues are present.

The 25-residue heterodimeric peptide AB compsed of peptide A disulfide-bridged to peptide B was synthesized using directed disulfide displacement and purified by HPLC. The homodimers CC and DD, randomly scrambled versions of peptides AA and BB, respectively, were prepared as controls. The sequences of these seven soluble peptides are shown in Table 1.

A competitive ELISA was used to examine the effect of each of these soluble peptides on the interaction of moFc$_\gamma$RII and IgG. Wells of a microtiter plate were coated with sFc$_\gamma$RII, a protein corresponding to the extracellular region of moFc$_\gamma$RII (Qu et al., 1988), which had been purified from the supernatants of CHO cells by affinity chromatography with Fabs from the antibody 2.4G2. The wells were then treated with immune complexes formed from the antibody ANO6 and the antigen DNP-HSA in the absence or presence of various concentrations of each peptide. Binding was detected by using horseradish peroxidase-conjugated goat anti-(mouse IgG) IgG as the secondary antibody.

The results of these assays are shown in Figure 4. The data shown are the averages of three scaled measurement sets. Each set was first background-corrected to account for absorbance due to the substrate buffer. To account for day-to-day variations in the absolute absorbance measurements, each set was separately averaged, and the relative values of the three averages were used to scale two of the data sets to the third. The three scaled data sets were then averaged, and the resulting data were normalized so that the initial point was equal to one.

Each of the seven soluble peptides partially inhibited the binding of immune complexes to immobilized sFc$_\gamma$RII (Figure 4). Peptides B and BB both inhibited the binding of mouse IgG1 immune complexes to immobilized sFc$_\gamma$RII at concentrations as low as 2 μM (Figure 4). These peptides exhibited very similar inhibition properties. The maximum inhibition was observed for concentrations at or above 20 μM and was about 52% for B and 65% for BB. Concentrations as high as 100 μM had no further effect on IgG1−sFc$_\gamma$RII binding. These results confirmed that the isolated 13-residue segment of moFc$_\gamma$RII (Cys^{153}−Lys^{165}) interacts with IgG1 but showed that peptide B lacks the full set of residues and/or the conformation required for total inhibition of IgG1−receptor binding.

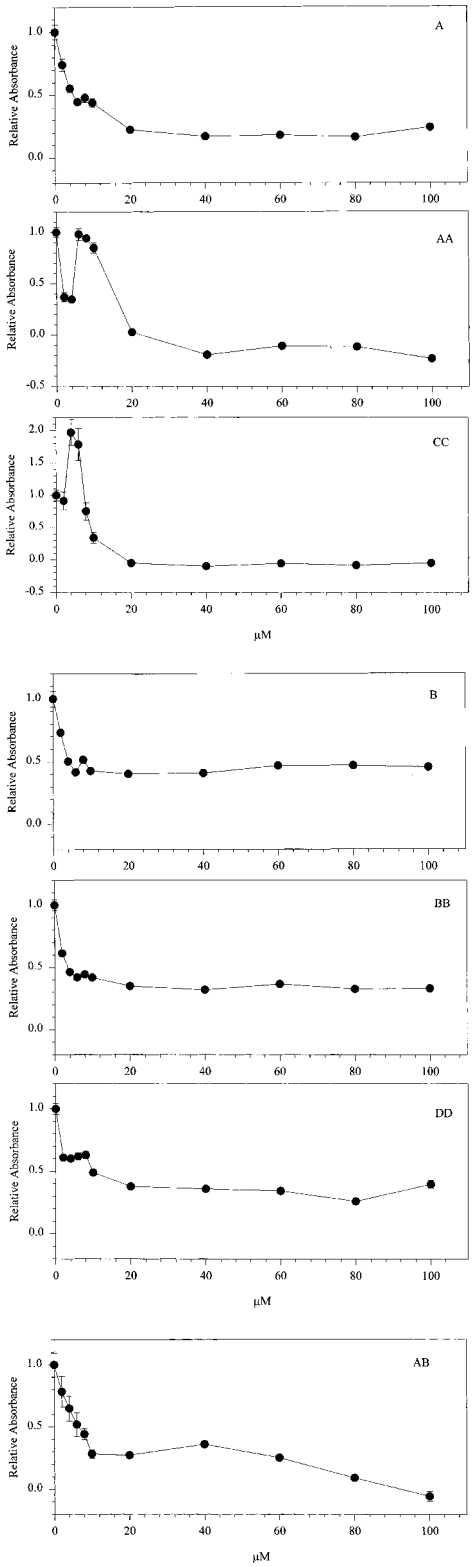

FIGURE 4: Competitive ELISA plots for the seven soluble peptides. The relative absorbance at 490 nm, which is proportional to the amount of the IgG1 immune complex bound to immobilized sFc$_\gamma$RII, is plotted against the micromolar concentration of peptide present. Panels A, B, AA, BB, AB, CC, and DD show inhibition plots for the corresponding peptides. Each point represents the average of three scaled measurement sets, and its error bar is the standard error of the mean. Each set was first background-corrected to account for absorbance due to the substrate buffer. To account for day-to-day variations in the absolute absorbance measurements, each set was separately averaged, and the relative values of the three averages were used to scale two of the data sets to the third. The three scaled data sets were then averaged, and the resulting data were normalized so that the initial point was equal to 1.

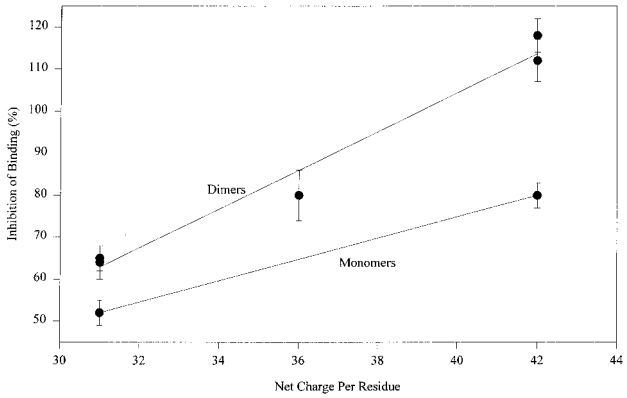

FIGURE 5: Correlation of peptide inhibition of binding with net peptide charge per residue. For each peptide, the percent inhibition of binding of immune complexes to immobilized sFc$_\gamma$RII (Figure 4) is plotted against the net charge per residue (Table 1). Each point is the average inhibition seen at 40−100 μM peptide, and the error bar is the standard error of the mean. The least-squares lines of best fit are shown for the two monomers (closed circles) and for the five dimers (closed squares).

The binding properties of peptides A and AA were quite different from each other and from those of peptides B and BB (Figure 4). Peptide A exhibited partial inhibition at concentrations as low as 2 μM and at 20−100 μM showed maximum inhibition of 80%. Interestingly, peptide AA at 2−4 μM partially inhibited the binding of immune complexes to sFc$_\gamma$RII but at 6−8 μM did not inhibit binding. A plausible explanation for this apparent lack of inhibition is that the homodimeric peptide AA binds to two immune complexes to produce larger complexes having increased multivalency and affinity for the sFc$_\gamma$RII-coated surface. At 10−20 μM, peptide AA partially inhibited IgG1−sFc$_\gamma$RII binding, and at 20−100 μM, it showed complete inhibition. Evidently, at a sufficiently high concentration, the homodimer AA no longer bridges two immune complexes.

As in native moFc$_\gamma$RII, Cys^{109} of peptide A and Cys^{153} of peptide B are joined by a disulfide bond in the heterodimer AB. As the concentration of peptide AB was increased from 2 to 10 μM, the inhibition of IgG1−sFc$_\gamma$RII binding increased linearly to about 80% inhibition (Figure 4). Above 10 μM, the inhibition of peptide AB slowly increased, peaked, and at 100 μM inhibition was complete. These results suggest that at concentrations below 10 μM peptide AB mainly interacts with the Fc region of IgG1 through its A chain. Above 10 μM, however, peptide AB also displays a weaker interaction through its B chain.

The importance of the order of the residues in peptides A and B was tested by measuring inhibition plots for sequence-scrambled (permuted) versions of homodimers AA (called CC) and BB (called DD). The scrambled peptides behaved very similarly to their unscrambled counterparts (Figure 4). This result suggests that the key features of peptides A, AA, B, BB, and AB that alter IgG1−Fc$_\gamma$RII binding are not their amino acid sequences but their amino acid compositions.

The degree of inhibition for the seven soluble peptides correlated with peptide charge as shown in Figure 5 and Table 1.

DISCUSSION

Pin peptide 108 exhibited significant affinity for immune complexes formed from the anti-DNP mouse IgG1 antibody ANO6 and the DNP-HSA antigen as well as for the

monomeric anti-moFc$_\gamma$RII rat antibody 2.4G2 (Figures 1 and 2). By analogy to structural models for human Fc$_\gamma$RII (Hulett et al., 1995), pin peptide 108 spans residues 108−119 in the B/C loop within the membrane-adjacent Ig domain of moFc$_\gamma$RII and contains residues that are adjacent to the Cys^{109}−Cys^{153} disulfide bond. Another pin peptide with significant affinity for immune complexes spanned residues 155−166 in the F/G loop, which are also adjacent to this disulfide bond.

Seven soluble peptide amides related to these pin peptides were synthesized by the solid-phase method. The moFc$_\gamma$RII peptides 108−119 and 153−165 were prepared as S-alkylated monomers (A, B), as disulfide-bridged homodimers (AA, BB), and as a disulfide-bridged heterodimer (AB). Scrambled versions of these homodimers (CC, DD) were also produced. These seven soluble peptides (Table 1) all inhibited the binding of the ANO6/DNP-HSA immune complexes to immobilized sFc$_\gamma$RII (Figure 4).

The net charge at pH 7.4 of peptide A is +5 and of peptide B is +4, which suggests that they interact with IgG1 by at least partially electrostatic interactions. This conclusion is consistent with the relationship between immune-complex binding and the net charge of the peptides on pins (Figure 3). In addition, for the seven soluble peptides, the percentage of maximum inhibition of binding increased as the net charge per residue increased (Figure 5). The lines through the points for the two monomeric peptides and for the five dimeric peptides have the same slope. The fact that IgG1−Fc$_\gamma$RII binding is enhanced at low ionic strength (Hsieh & Thompson, 1995) is also consistent with a major role for electrostatic binding of IgG1 to moFc$_\gamma$RII. In future studies, it will be of interest to further define the role of electrostatics in IgG1−moFc$_\gamma$RII binding by examining the behavior of peptides in which the uncharged residues are replaced with ones not present in the native peptides, and in which the lysine and arginine residues are replaced with arginine and lysine residues, respectively.

It is highly likely that the residues in peptides A and B are part of the Fc binding region in the native moFc$_\gamma$RII protein. Two forms of this receptor (Ly-17.1 and Ly-17.2) have been identified (Hulett & Hogarth, 1994) based on a genetic polymorphism. Isoform Ly-17.1 has Pro^{116} and Gln^{161}, whereas isoform Ly-17.2 has Leu^{116} and Leu^{161}. These residues are located in the membrane-adjacent Ig domain of Fc$_\gamma$RII. Antibodies specific for the Ly-17.2 antigen inhibit both Fc-mediated IgG−receptor binding and the Fab-mediated binding of 2.4G2, a rat monoclonal antibody that is specific for the mouse Fc$_\gamma$RII receptor and that blocks IgG−receptor binding (Hibbs et al., 1985). These results suggest that mouse IgG binds to the membrane-adjacent Ig domain of Fc$_\gamma$RII, which is consistent with our finding that peptides A and B from this domain alter IgG−receptor binding. Furthermore, the result that one or both of the residues at positions 116 and 161 play an important role in binding is consistent with the sequences of peptide A, which contains Leu^{116}, and peptide B, which contains Leu^{161}.

Peptides A and B can also be compared with published results for human Fc$_\gamma$RII. In one study (Hulett et al., 1993), chimeric receptors generated from human Fc$_\gamma$RIIa and human Fc$_\epsilon$RI localized the IgG binding site to a 16-residue segment (145−169) in the membrane-adjacent domain. By using site-directed mutagenesis, this segment was later localized to eight residues (154−161) of the F/G loop (Hulett et al., 1994). Replacement of either Ile^{155} or Gly^{156} by alanine prevented IgG binding, but substitution of either Leu^{159} or Phe^{160} by alanine enhanced IgG binding. These results are consistent with several of the residues in peptide B (153−165) being part of the Fc binding site in the mouse receptor. Additional chimera studies have identified two other segments (Ser^{109}−Val^{116}, Ser^{130}−Thr^{135}) in the membrane-adjacent domain of human Fc$_\gamma$RII that contribute to IgG binding (Hulett et al., 1995). The 109−116 segment of the B/C loop is contained within peptide A (108−119).

The F/G loop of the human Fc receptor is thought to be primarily responsible for IgG binding with the B/C loop playing a peripheral role. In contrast, our results for the mouse Fc receptor suggest that the B/C loop peptide A binds more strongly to IgG than does the F/G loop peptide B. Given the structural homology of the Fc$_\gamma$RII receptors in mouse and human, it is interesting that the contributions of the B/C and F/G loops to IgG binding may be reversed.

Peptides identical to or similar to the ones identified in this work might have significant clinical importance because of their ability to inhibit the binding of immune complexes to Fc$_\gamma$RII. In addition, dimeric peptides AA and CC can increase immune-complex binding at moderate concentrations but completely inhibit binding at high concentrations. If these synthetic moFc$_\gamma$RII peptides can facilitate immune-complex binding to cell surface Fc$_\gamma$RII *in vivo*, they might be useful for reducing inflammation, as previously seen for soluble recombinant human Fc$_\gamma$RII (Ierino et al., 1993).

ACKNOWLEDGMENT

We thank J. C. Unkeless, Z. Qu, J. D. Odin, and J. D. Glass of Mt. Sinai School of Medicine for CHO cells which secrete sFc$_\gamma$RII; H. M. McConnell of Stanford University for ANO6 hybridomas; B. Diamond of the Albert Einstein College of Medicine for 2.4G2 hybridomas; C. L. Poglitsch and D. Gesty-Palmer for biochemical preparations; G. Vasquez and R. J. Pettis for assistance with peptide synthesis and HPLC; J. G. Goldsmith of the University of South Carolina at Aiken for assistance with automated computer analysis of peptide charge; and R. J. Pettis, L. Chen, E. D. Sheets, and D. Gesty-Palmer for helpful discussions.

REFERENCES

Burns, J. A., Butler, J. C., Moran, J., & Whitesides, G. M. (1991) *J. Org. Chem. 56*, 2648.

Burton, D. R. (1985) *Mol. Immunol. 22*, 161.

Gesty-Palmer, D., & Thompson, N. L. (1997) *J. Mol. Recognit.* (in press).

Geysen, H. M., Meloen, R. H., & Barteling, S. J. (1984) *Proc. Natl. Acad. Sci. U.S.A. 81*, 3998.

Geysen, H. M., Rodda, S. J., Mason, T. J., Tribbick, G., & Schoofs, P. G. (1987) *J. Immunol. Methods 102*, 259.

Habeeb, A. F. S. A. (1972) *Methods Enzymol. 25*, 457.

Hibbs, M. L., Hogarth, P. M., & McKenzie, I. F. C. (1985) *Immunogenetics 22*, 335.

Hibbs, M. L., Classon, B. J., Walker, I. D., McKenzie, I. F. C., & Hogarth, P. M. (1988) *J. Immunol. 140*, 544.

Hsieh, H. V., & Thompson, N. L. (1995) *Biochemistry 34*, 12481.

Hulett, M. D., & Hogarth, P. M. (1994) *Adv. Immunol. 57*, 1.

Hulett, M. D., McKenzie, I. F. C., & Hogarth, P. M. (1993) *Eur. J. Immunol. 23*, 640.

Hulett, M. D., Witort, E., Brinkworth, R. I., McKenzie, I. F. C., & Hogarth, P. M. (1994) *J. Biol. Chem. 269*, 15287.

Hulett, M. D., Witort, E., Brinkworth, R. I., McKenzie, I. F. C., & Hogarth, P. M. (1995) *J. Biol. Chem. 270*, 21188.

Ierino, F. L., Powell, M. S., McKenzie, I. F. C., & Hogarth, P. M. (1993) *J. Exp. Med. 178*, 1617.
James, J. A., & Harley, J. B. (1992) *J. Immunol. 148*, 2074.
Kemeny, D. M. (1991) *A practical guide to ELISA*, Pergamon Press, Oxford.
Kinet, J. (1989) *Cell 57*, 351.
Leahy, D. J., Rule, G. S., Whittaker, M. M., & McConnell, H. M. (1988) *Proc. Natl. Acad. Sci. U.S.A. 85*, 3661.
Mellman, I., & Plutner, H. (1984) *J. Cell Biol. 98*, 1170.
Mellman, I., Koch, T., Healey, G., Hunziker, W., Lewis, V., Plunter, H., Miettinen, H., Vaux, D., Moore, K., & Stuart, S. (1988) *J. Cell Sci., Suppl. 9*, 45.
Pisarchick, M. L., & Thompson, N. L. (1990) *Biophys. J. 58*, 1235.
Poglitsch, C. L., & Thompson, N. L. (1990) *Biochemistry 29*, 248.
Qu, Z., Odin, J., Glass, J. D., & Unkeless, J. C. (1988) *J. Exp. Med. 176*, 1195.
Ravetch, J. V., & Kinet, J. (1991) *Annu. Rev. Immunol. 9*, 457.
Ravetch, J. V., Luster, A. D., Weinshank, R., Kochan, J., Pavlovec, A., Portnoy, D. A., Hulmes, J., Pan, Y. E., & Unkeless, J. C. (1986) *Science 234*, 718.
Shaw, D. C., Harris, D. L., He, X., Oster, J. A., Montogomery, D. L., Ely, K. R., & Edmundson, A. B. (1987) *Mol. Immunol. 24*, 267.
Unkeless, J. C. (1979) *J. Exp. Med. 150*, 580.
Unkeless, J. C., Fleit, H., & Mellman, I. S. (1981) *Adv. Immunol. 31*, 247.
Williams, A. F., & Barclay, A. N. (1988) *Annu. Rev. Immunol. 6*, 381.

BI961564B